

Kinetics of intermediate-mediated self-assembly in nano-sized materials: a generic model

James F. Lutsko,^{1,*} Vasileios Basios,¹ Grégoire Nicolis,¹ Tom P. Caremans,² Alexander Aerts,² Johan A. Martens,² Christine E. A. Kirschhock,² and Titus S. van Erp^{2,†}

¹*Center for Nonlinear Phenomena and Complex Systems CP 231,
Université Libre de Bruxelles, Blvd. du Triomphe, 1050 Brussels, Belgium*

²*Center for Surface Chemistry and Catalysis, K. U. Leuven,
Kasteelpark Arenberg 23, 3001 Leuven, Belgium*

(Dated: March 30, 2010)

Abstract

We propose in this paper a generic model of a non-standard aggregation mechanism for self-assembly processes of a class of materials involving the mediation of intermediates consisting of a polydisperse population of nano-sized particles. The model accounts for a long induction period in the process. The proposed mechanism also gives insight on future experiments aiming at a more comprehensive picture of the role of self-organization in self-assembly processes.

I. INTRODUCTION

Nanophase materials are of key importance in a variety of fields from molecular and cellular biology to technological innovation. They also pose major theoretical challenges in view of their multiple scale dynamics, whereby microscopic level processes determine macroscopic properties through the growth of initial fluctuations favoring in some way the specific material that will eventually emerge from synthesis. This switches on, in turn, a variety of self-organization phenomena associated with the coexistence of competing pathways.

The processes we investigate in this work involve two steps. First, an initial species, N , is able to agglomerate into an intermediate form, X . We will primarily envisage the increase/decrease in the amount of X as being due to the attachment/detachment of units of N although more complex dynamics might be relevant in some cases. We expect that N and X will reach an equilibrium in a relatively short time. The second step of the process is the self-assembly of the final product, S , from X . By “self-assembly” we imagine that the units of X must not only join together to form S , but must undergo some sort of internal transition (such as a restructuring) which is quite slow. One of the main points of this work is to show that simply assuming a long characteristic time (i.e. a small rate constant) for this internal transition is not sufficient to give a long induction time. However, by including cooperativity - whereby the nascent S material templates or catalyzes the internal transition - arbitrarily long induction times can be achieved. A mathematical model of the contribution of cooperativity will be developed based on general physical considerations of how the process must proceed.

The need to synthesize intermediate substances prior to the material of interest is also a well known phenomenon in chemistry, where it is typically also reflected by the appearance of an induction period¹⁻⁵. Hierarchical self-assembly is also ubiquitous in biology. In particular, in a series of papers on the polymerization and crystallization of sickle cell Hemoglobin (HbS) –an issue of crucial importance for the pathophysiology of sickle cell anemia– it has been shown that metastable dense liquid clusters serve as precursors to the ordered nuclei of the HbS polymerization⁶⁻⁸. Induction times causing time delay have been observed and analyzed during this non-standard nucleation process of the HbS polymers. More generally, it is now known that homogeneous nucleation -most notably in nanophase materials such as proteins but apparently even in simple fluids - can involve a two step process starting with

the formation of more structured liquid-like droplets and/or clusters⁸⁻¹⁰ from the solution followed by the development of crystalline order^{11,12}. Here, the material in solution can be viewed as the population N of our scheme, the dense-liquid phase as the intermediate, X, and the solid as S. Cooperativity is again responsible for the induction period and time delays during the subsequent ordering corresponding to the processes $N \rightarrow X$ and $X \rightarrow S$.

A class of nanophase materials in which self-assembly appears to be accompanied by a rich variety of unexpected behaviors are synthetic zeolites^{11,13-17} which find nowadays applications in a broad range of areas such as heterogeneous catalysis, petroleum refining, and microelectronics^{18,19}. In the context of zeolite formation mechanism, Silicalite-1 type zeolite²⁰ in particular has been the subject of numerous studies²¹⁻³⁶.

The starting point of Silicalite-1 synthesis is a suspension of 3 nm silicate nanoparticles²³. The first period of ageing, at room or elevated temperature, is characterized by a rapid evolution of these nanoparticles. During this period, the average nanoparticle diameter increases to a slightly larger value of 5-6 nm^{22,29,31,36}. On a structural level, the nanoparticle silicate network condenses, i.e. additional siloxane (Si-O-Si) bonds are formed^{32,35,36}. Subsequently, still larger particles start growing, ultimately resulting in Silicalite-1 zeolite crystals. Convincing evidence shows that Silicalite-1 crystals grow by aggregation of the 5-6 nm nanoparticles³¹. It was proposed that a fraction of the condensed 5-6 nm nanoparticles develops a zeolite crystalline framework. These intermediate nanoparticles can be identified as "nuclei" for zeolite crystal growth by nanoparticle aggregation³¹. The picture is then one of nanoparticles N giving rise to intermediates X which, in turn, form the (zeolite-crystalline) solid S, as illustrated in Fig. 1 Recent experimental liquid state ²⁹Si NMR and pH results³⁶ of Silicalite-1 zeolite crystallization are presented and described in Fig 2.

Fig 2-ab shows the experimental distribution of silicon among different species in suspension, determined with liquid state ²⁹Si NMR. There is a long induction period during which the amount of nanoparticles varies slowly, followed by a rather abrupt transition towards an equilibrium state dominated by zeolite crystalline material (solid). Because nanoparticles N and intermediates X have similar size NMR cannot distinguish between these two species. The rapid condensation of nanoparticle framework in the initial stage, resulting in the formation of intermediates, is evident from the silicon connectivity distribution (Fig 2-d) and the corresponding increase of the suspension pH (Fig 2-c). Upon transition to crystalline material, the pH shows a second increase.

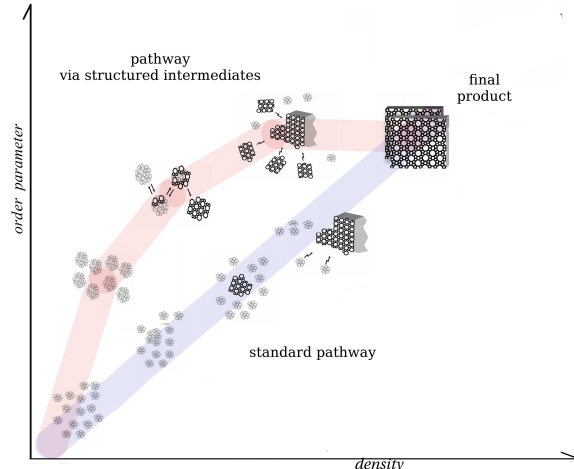


FIG. 1: A schematic demonstration of multistep versus standard synthetic pathways in a two-order parameter space accounting for the presence of partially structured intermediates.

Notice that during the later stages of crystallization, other mechanisms, such as Ostwald ripening, acting on the already formed aggregates are likely to take over as dominant crystallization mechanism.

In view of the foregoing we argue that a timescale separation and the appearance of long quasi-stationary plateaus is likely to be a generic property of large classes of synthetic processes. One of the main goals of this article is the theoretical explanation of the mechanisms underlying these phenomena. We establish a generic theoretical model which captures the main features of self-organization in the process of multi-step nucleation and growth. Specifically, we show how the combination of intermediate steps in self-assembly, together with first-order nucleation and cooperativity, in the form of growth controlled by the available surface area of the product, can explain the long induction times often observed in these processes. For the particular case of zeolites, our model is intended to sort out the basic microscopic mechanisms that control the nucleation and growth of the final crystalline product. This can have some practical repercussions in not only eliminating superfluous conjectures that could be entertained in the absence of theoretical input, but also in further designing targeted and better controlled experiments.

The article is organized as follows: In Section 2, we outline the proposed mechanisms for self-organization incorporated in our mathematical models. In Section 3 we develop a simple phenomenological model based on the assumption of cooperative behavior which reproduces

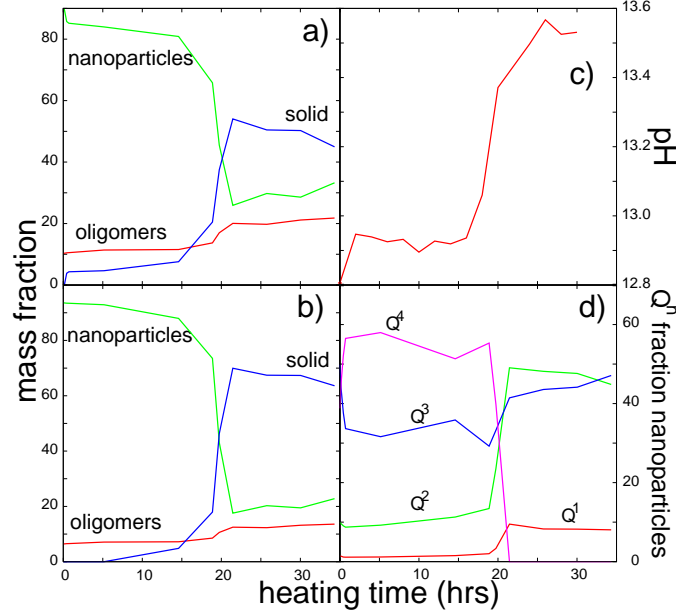


FIG. 2: (Color on line) Liquid state ^{29}Si NMR and pH results from Ref. [36]. (ab) Evolution of nanoparticles (N and similarly sized X particles), oligomers and NMR- undetected phase (denoted as "solid"). The undetected phase consists of large particles, i.e. crystalline solid (S) and possibly a fraction of intermediates (X particles that are considerably larger than nanoparticles), that fall outside the NMR detection limit. The oligomers are an additional group of smaller silicate species, but their presence is assumed to be of only secondary importance for the crystal growth. Panel-a: direct NMR results obtained with a short delay time of 7 sec between radiofrequency pulses in the NMR experiment. The process shows two-step evolution. The first step ($< 1\text{hr}$) indicates the formation of intermediate species. Subsequently, there was a long induction period during which the amount of nanoparticles varied slowly, followed by a rather abrupt transition towards an equilibrium state dominated by zeolite crystalline material. It is noted that in the original publication, these NMR data were corrected to account for a longer NMR delay time of 92 s (Panel-b), based on measurement of the unheated sample³⁶. The correction resulted in quantitatively more reliable populations but the initial step was suppressed. The two-step evolution was also evident from measurements of the suspension pH (panel-c) and the connectivity of the nanoparticle framework (panel-d). The connectivity is expressed as Q^n fractions, where Q^n stands for a silicon atom connected to $n = 1 - 4$ neighboring silicons via siloxane bonds. The disappearance of the Q^4 fraction might indicate a depletion of the more structured X-particles.

much of the qualitative behavior summarized above. A more microscopic and mechanistic model is presented in Section 4 and shown to describe the generic qualitative features of recent observations and lead to a prediction regarding the distribution of cluster sizes. The main conclusions are summarized in Section 5.

II. THE MECHANISMS FOR SELF-ORGANIZATION AND THEIR MODELING

In this section we outline the construction of mathematical models capable of quantifying the mechanisms summarized in the Introduction and, in particular, the presence of multiple time scales and the existence of a long induction period. The models to be developed are articulated around three basic steps which account for the self-organizing behavior.

- (a) Equilibration between nanoparticles and intermediates. This part of the dynamics will depend on the details of specific systems. Here, we will model it as a globally autocatalytic process whereby nanoparticles and intermediates interact to form new intermediates while depleting the nanoparticle population. The rationale behind this assumption is that in the particular case of zeolites, the intermediate is not a single species but, rather, it is believed to consist of a population of structures of various sizes^{24,36}. We assume that the dominant mechanism for conversion of nanoparticles into intermediates is growth of smaller intermediates via aggregation of nanoparticles, i.e., via an autocatalytic mechanism. It would be possible to include nucleation of new intermediates, but it seems likely that growth will be the dominant process so that, for simplicity, nucleation can be neglected. It is assumed that at the beginning, a small population of intermediates is already present due, e.g., to thermal fluctuations. Obviously, for other systems, such as proteins, first-order reactions characteristic of nucleation would be more appropriate.
- (b) Initial formation of final product. At some point, a stable cluster of S must be formed which will then proceed to grow and we assume that the long plateau referred to earlier is a measure of the time required for this to occur. In a simple fluid this would be recognized as a nucleation phenomena³⁷ which is typically modeled as a probabilistic process occurring with a probability per unit time proportional to the supersaturation. In the case of more complex materials, it may be that the intermediates must pass

through multiple structural phases or that some other type of transformation of the intermediates is necessary before stable clusters of final product can form. It might be more appropriate in this case to speak of self-assembly rather than nucleation³⁸. Nevertheless, we will assume that this complex microscopic process can be crudely described in the same terms as nucleation in a simple fluid.

- (c) Growth and Cooperativity. Once the product begins to form, the speed of the process increases dramatically. This is a signal of cooperative behavior whereby the presence of some product accelerates the formation of new product. One possibility is that this is simply due to the growth of the clusters once they are formed. In simple fluids, secondary nucleation - the nucleation of new crystals on the surfaces of existing crystals - also occurs and can speed the formation of crystals³⁹. In more complex materials, if the intermediates must pass through different phases, then a growing cluster could also catalyze that process thereby accelerating cluster formation. We will not try to distinguish these different mechanisms but will simply account for an acceleration of the rate of cluster formation due to the presence of existing product.

We will discuss the implementation of this phenomenological framework in two stages. First, we translate it into a crude phenomenological model which serves to illustrate the general ideas. Then, we describe a more microscopic, mechanistic approach that leads to similar results and that has the advantage of being less ad hoc and of making further predictions.

III. PHENOMENOLOGICAL MODEL

We consider a closed reactor initially containing nanoparticles, N , present in abundance, along with an intermediate (more ordered and larger) species, X , present in small amounts. Rather than forming the product, S , directly, the N particles first accumulate to form the intermediate X . In fact, the single intermediate in the model represents a spectrum of species. These species undergo reactions which convert from one type of intermediate to another, but this will not be modeled here. Instead, we only track the net mass of intermediates which increases by consuming nanoparticles. In certain cases, such as zeolite crystallization, it is believed that the intermediates are the only species possessing the necessary structure

that allows them to bind together to form solid³⁶. For this reason, we restrict our analysis to the sequence $N \rightarrow X \rightarrow S$ and do not consider possibilities such as direct conversion of nanoparticles into solid which may be of relevance to other processes. Such alternatives could easily be included within the framework described below. The N to X transition is taken to be an autocatalytic process of order higher than one, with a rate ν_1 depending on the abundance of both N and X. Furthermore, in agreement with available data it is stipulated that the X particles accumulate to give rise to S. The X to S transition occurs at a rate, ν_2 , that describes two processes. First, as discussed above, the initially slow formation of stable clusters is modeled as a probabilistic event occurring at a rate that depends on the supersaturation. Then, as the final product is formed, the rate increases due to cooperativity. Thus, the total rate of formation of the product will depend on the concentration of intermediates and of the product itself. To avoid the presence of stoichiometric coefficients we choose to work with the mass fractions n , x and s of N, X and S particles respectively since by mass conservation the rate of loss of n in the N to X transition will then necessarily be equal to the rate of growth of x , etc. We obtain in this way the following three coupled differential equations,

$$\begin{aligned}\frac{dn}{dt} &= -\nu_1(n, x) \\ \frac{dx}{dt} &= \nu_1(n, x) - \nu_2(x, s) \\ \frac{ds}{dt} &= \nu_2(x, s),\end{aligned}\tag{3.1}$$

the corresponding kinetic scheme being



Notice the conservation condition

$$n + x + s = \text{constant}\tag{3.3}$$

This relation does not involve the mass fraction of oligomers as they are believed to play a secondary role in the process and are therefore neglected³⁶.

To illustrate this behavior, we choose to model the rate ν_1 as a Verhulst type growth process^{1,40},

$$\nu_1(n, x) = k_1 nx - k_2 x^2\tag{3.4}$$

whereby nanoparticles and intermediates react to produce more intermediate species. Notice that balance is achieved when $n = \frac{k_2}{k_1}x$ so that the ratio of rate constants can be fixed by the quasi-equilibrium level of the mass fractions which occur at short times. The value of, say k_1 is then determined by the time the system takes to reach this quasi-stationary state. Thus, these parameters are completely determined by the short-time behavior of the system.

The rate ν_2 is broken into two parts: $\nu_2(x, s) = \nu_{21}(x) + \nu_{22}(x, s)$. The first part depends only on the amount of X present and represents the nucleation/self-assembly process. For this, we take the simplest reasonable form, $\nu_{21}(x) = k_3(x - x_0)$, where x_0 is the equilibrium concentration of X so that $x - x_0$ represents the supersaturation. The second part of the rate represents the effect of cooperativity. We have not found it possible to model the behavior observed in the zeolite data using higher order terms involving only the concentration of intermediates. Instead, we have found it necessary to model this as an enhancement of the nucleation rate that depends on the amount of product already formed, $\nu_{22}(x, s) = k_3\alpha s^\mu(x - x_0)$. In the following we always assume that $x_0 = 0$ which implies that once the product is formed from X, it will not dissolve again.

Putting these pieces together, the phenomenological model is given by

$$\frac{dn}{dt} = -k_1nx + k_2x^2 \quad (3.5)$$

$$\begin{aligned} \frac{dx}{dt} &= k_1nx - k_2x^2 - k_3x(1 + \alpha s^\mu) \\ \frac{ds}{dt} &= k_3x(1 + \alpha s^\mu) \end{aligned} \quad (3.6)$$

Long induction times are expected to arise when the cooperative part of the process is slow, which is to say that $k_3 \ll k_1, k_2$. In this case, the model exhibits dynamics on two different time scales: at short times, the cooperative part can be neglected with the result that $c = n + x$ is conserved (since virtually no product forms) and the model can be integrated to give $n(t) = c - x(t)$ and

$$x(t) = \frac{k_1cx(0)}{k_1c - (k_1 + k_2)x(0)(e^{-k_1ct} - 1)} \quad (3.7)$$

For $k_1ct \gg 1$, this leads to an equilibrium with $x = \frac{k_1c}{k_1 + k_2}$. Thus, assuming that c is on the order of 1, we find equilibration on a time scale determined by k_1 and with relative fractions of material in the form of N and X determined by k_2 . This short-time equilibration is expected to describe the beginning of the self-assembly process when materials are first mixed, heat is first applied, etc.

At longer times, nucleation and cooperativity contribute causing the system to evolve away from the short-time steady state. There is then a new, long-time steady state in which $x \rightarrow 0$. At intermediate times, the model must be solved numerically. Figure 3 shows the result of such a solution starting with initial conditions $x(0) = 10^{-4}$ and $n(0) = 1 - x(0)$, corresponding to an initial state in which almost all the mass is in the form of nanoparticles. We take $k_2 = 9k_1$ so that the short-time equilibration leads to $n = 0.9$ and $x = 0.1$. To illustrate the presence of a long induction time, the value $k_3 = 0.002k_1$ was used so that if $1/k_1$ is on the order of a minute, then significant self-assembly of the final product only occurs after a time on the order of $1/k_3$ or about 8 hours. The remaining constants, α and μ , primarily control the speed with which the system makes the transition from its short-time steady state to the final long-time steady state. These values were chosen somewhat arbitrarily to be $k_3\alpha = k_1$ and $\mu = 1.75$. The figure shows that after a rapid equilibration, the system experiences a long period of slow nucleation that is followed by a rapid transition to the final steady state. The final transition begins to occur around $k_1t \sim 250$ correspond to $t \sim 4\text{hr}$ for $k_1 = 1/\text{minute}$. Qualitatively, this behavior is similar to that observed in the zeolite experiments of Aerts et al³⁶ (compare to Fig. 2).

Finally, we note some specific features of this model that are motivated by the experimental data shown in Fig. 2. First, there is no evidence of nucleation of intermediates from nanoparticles. This is in part based on the fact that the nanoparticle concentration reaches a finite plateau even though the intermediates are depleted. Nucleation may a priori occur on much longer timescales than that of the experiment in which case the observed plateau is only quasi-stationary. This would then suggest adding a term $-k_4n$ to the equation for dn/dt and a corresponding term in the equation for dx/dt . However, the rate constant would be very small thus justifying our neglect of this term on these timescales. Second, the conversion of intermediates to solid is irreversible. This is motivated by the fact that dissolution of zeolite crystals in alkaline medium does not lead to the extraction of silicate species of the size of nanoparticles or larger⁴¹ (which also explains the depletion of X (see fig. 2d)). This leaves open the possibility of an equilibration between the solid and the oligomers, but, as can be seen from Fig. 2, such a reaction, if it exists, is of secondary importance and must take place on longer time scales than that of the formation of solid from nanoparticles. Besides, the fact that the crystals eventually grow to macroscopic size suggests that the formation of solid is, for all practical purposes, irreversible.

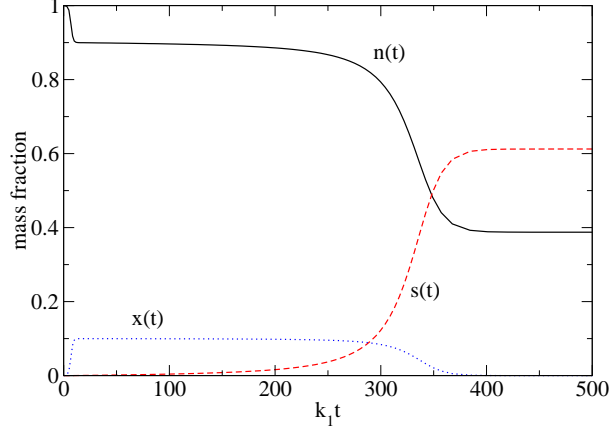


FIG. 3: (Color on line) Solution of the phenomenological model, Eq.(3.5), with the rate constants given in the text. The full line is the mass fraction of the nanoparticles, the dotted line is that of the intermediates, $x(t)$, and the broken line is that of the final product, $s(t)$

IV. A MORE MICROSCOPIC APPROACH

Having shown that the combination of nucleation/self-assembly and cooperativity appears to give a reasonable description of the mechanisms of self-assembly, we now describe a more concrete realization of this picture. It is expected that assumptions made here are both more physically plausible than those made above and more intuitively appealing. They are:

1. The $N \rightleftharpoons X$ reaction is the same as assumed in the previous section.
2. Formation of new stable clusters of final product occurs at a rate proportional to the supersaturation.
3. The initial size of a stable cluster is always the same.
4. Once formed, clusters grow at a rate proportional to their surface area and to the supersaturation.
5. All clusters are geometrically identical.
6. The formation rate is enhanced by a factor proportional to the surface area of the existing clusters and to the supersaturation.

Assumptions 1 and 2 are the same as made previously. Assumption 3 is perhaps the most problematic: in a simple fluid it might be justified on the grounds that growing clusters are

presumed to start out as a stable cluster which has a fixed size (at least for a given supersaturation). This may be true here. If not, it can be imagined that there is a distribution of initial cluster sizes and that we are describing an average over an ensemble of such clusters. Assumption 4 explicitly introduces cluster growth which was neglected in the previous section (or, at least, it was crudely lumped together with cooperativity). Assumption 5 is merely a convenience so that we can be specific concerning geometric factors such as the ratio of volume to surface area of a cluster. Assumption 6 seems the simplest, physically plausible way to introduce the idea of cooperativity.

These models involve the area, A , and mass or, equivalently, volume, V , of growing clusters. For spherical clusters, we of course expect that $A \sim R^2, V \sim R^3$ where R is the radius. In fact, these scaling relations should hold for three dimensional growth, with R some measure of linear size, regardless of the precise shape of the clusters. However, other modes are possible and are of relevance for growth of some protein molecules. For example, suppose that the cluster has the shape of a cylinder with crosssectional area πr^2 and length L . Quasi-one-dimensional growth would occur if the cylinder lengthens with constant cross section. This would involve attachment on the flat faces so that the active growth area would be $2\pi r^2$, a constant, while the volume would be $\pi r^2 L(t)$. Quasi-two-dimensional growth would occur if attachment happened on the curved part of the cylinder so that the crosssectional area increases with time while the length remains constant. Then, the active growth area would be $2\pi r(t) L$ and the volume $\pi r^2(t) L$. All of these cases can be summarized by the general scaling $A = G_A R^{D-1}, V = G_V R^D$ where R is the appropriate linear length scale and G_A and G_V are constant geometric factors. We will use this as our general model with the additional provision that D is an integer. We therefore rule out fractal growth patterns which could a priori be treated within our general framework but which do not admit of the mathematical simplifications we utilize below.

To translate this into a mathematical model for growth, some new quantities must be defined. Let $\mathcal{N}(t)$ be the number of clusters growing at time t and let $m(t, t')$ be the mass, at time t , of a cluster nucleated at time t' . Note that by assumption 3, $m(t, t) = m_0$ for some constant m_0 . Finally, the total mass of nanoparticles, intermediates, solid and oligomers is denoted M , and is a constant throughout the experiment. The total mass of solid at time t , $M_s(t)$, is simply given by a sum over the masses of all clusters present at time t . A cluster at time t has mass $m(t, t')$ if it was nucleated at time t' . The number nucleated at time t' is

simply $\frac{d\mathcal{N}(t')}{dt'}dt'$ so,

$$s(t) = M^{-1} \int_0^t m(t, t') \frac{d\mathcal{N}(t')}{dt'} dt' \quad (4.8)$$

where we assume that there is no final product present at the beginning of the experiment, $s(0) = 0$. Thus, based on assumption 4, the mass of a cluster grows as

$$\begin{aligned} \frac{dm(t, t')}{dt} &= k_g x A(t, t') \\ m(t, t) &= m_0 \end{aligned} \quad (4.9)$$

for some constant, k_g . Finally, the rate of appearance of new clusters is the sum of a nucleation-like term proportional to the supersaturation (assumption 2) and a cooperative term proportional to the total area of the clusters (assumption 6),

$$\frac{d\mathcal{N}(t)}{dt} = M k_n x + k_a x \int_0^t A(t, t') \frac{d\mathcal{N}(t')}{dt'} dt' \quad (4.10)$$

Note that we include a factor of the total mass in the nucleation term. This is because the number of clusters is an extensive quantity - as is the total area calculated in the second term. The number of nuclei generated per unit time must also be extensive, hence the factor of the mass.

At this point, the model seems much more complicated than the phenomenological model given above. However, after some simple manipulations (see Appendix), it can be described by a set of three first order differential equations which uses the same number of parameters as in the phenomenological model:

$$\begin{aligned} \frac{dn}{dt} &= -k_1 n x + k_2 x^2 \\ \frac{dx}{dt} &= k_1 n x - k_2 x^2 - \gamma x \frac{d\tilde{s}(u)}{du} \\ \frac{du}{dt} &= \gamma x \end{aligned} \quad (4.11)$$

Here, $u(t)$ is an auxiliary function with the initial condition $u(0) = 0$. The mass fraction of S is given by $s(t) = \tilde{s}(u(t))$ where

$$\tilde{s}(u) = \left(1 + \frac{D}{\alpha}\right) \sum_{i=1}^D a_i \exp(\lambda_i u) - D \frac{\beta}{\alpha} u \quad (4.12)$$

The constants λ_i are the roots of the D -th order equation

$$0 = \lambda^D - \alpha \sum_{j=1}^D \frac{(D-1)!}{(D-j)!} \lambda^{D-j} \quad (4.13)$$

while the coefficients a_i are

$$\begin{aligned} a_i &= \beta \frac{1}{2\lambda_i - \lambda_1 - \lambda_2}, \quad D = 2 \\ a_i &= \beta \frac{\alpha - \sum_{j \neq i} \lambda_j}{\prod_{j \neq i} (\lambda_i - \lambda_j)}, \quad D = 3 \end{aligned} \quad (4.14)$$

The case of general values of D is discussed in the Appendix. All of this is written in terms of the two dimensionless constants

$$\alpha = \frac{Dk_a m_0}{k_g}, \quad \beta = \frac{m_0 D G_V \rho R_0 k_n}{G_A k_g} \quad (4.15)$$

and the rate constant

$$\gamma = \frac{k_g G_A}{D R_0 \rho G_v} \quad (4.16)$$

where $m_0 = \rho G_V R_0^D$. Thus, despite the fact that the physical model involves 3 parameters, k_g, k_n and k_a , as well as the initial mass of a stable cluster, m_0 , and the total mass M and the density ρ , the data can be fit with only three parameters, α, β and γ , which is no more than the phenomenological model.

The present model is now written in terms of rate equations which are exactly equivalent to eqns (4.8-4.10). Still, it does not have the same form as the phenomenological model proposed in the previous Section. It is, however, possible to make a correspondence between them. Since both the mass fraction of S , $s(t)$, and the auxiliary variable $u(t)$ increase monotonically with time, and since they are related by a simple algebraic equation, eqn (4.12), we can imagine inverting that equation to get u as a function of s . An analytic inversion is not possible but for small u and s , this can be done perturbatively giving u as a power series in s . (See the Appendix for details.) Substitution into eqn (4.11) and specializing to $D = 3$ gives

$$\begin{aligned} \frac{dn}{dt} &= -k_1 n x + k_2 x^2 \\ \frac{dx}{dt} &= k_1 n x - k_2 x^2 - \beta \gamma x \left(1 + \frac{\alpha + 3}{\beta} s - \frac{\alpha + 3}{2\beta^2} s^2 + \dots \right) \\ \frac{ds}{dt} &= \beta \gamma x \left(1 + \frac{\alpha + 3}{\beta} s - \frac{\alpha + 3}{2\beta^2} s^2 + \dots \right) \end{aligned} \quad (4.17)$$

which is very similar to the phenomenological model except that the single term s^μ is replaced by an infinite series in s . Thus the adjustment of μ is seen as a way of accounting for the fact that the infinite sum is being approximated by a single term.

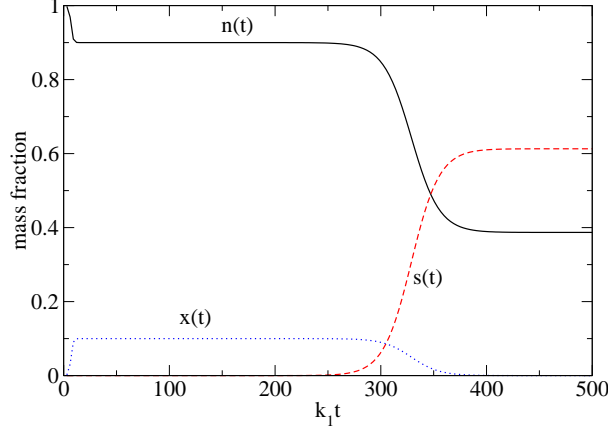


FIG. 4: (Color on line) Solution of the microscopic model, Eq.(4.11), (lines) with the rate constants given in the text. The full line is the mass fraction of the nanoparticles, the dotted line is that of the intermediates , $x(t)$, and the dashed line is the mass fraction of the solid, $s(t)$.

Figure 4 shows the result of a numerical solution of the model, Eq.(4.11). The constants k_1 and k_2 have the same values as used previously. The other constants, $\alpha = 8750$, $\beta = 1.67 \times 10^{-3}$ and $\gamma = 6.55 \times 10^{-5}k_1$, were chosen to give approximately the same point of crossing of the curves and similar final states as seen in the phenomenological model. In this case, the plateau resulting from the long induction time is even more pronounced and the transition to the steady state is even sharper than in the phenomenological model.

To test whether or not cooperativity is really required, we have attempted to model similar behavior with $k_a = 0$. Typical results are shown in Fig. 5. In this case, there are only two parameters and we find that it is not possible to simultaneously capture the long plateau up to $k_1 t \sim 200$ and to capture the crossing of the curves at about $k_1 t \sim 310$. Furthermore, in contrast to both the data and the model with cooperativity, the mass fractions do not show plateaus at long times. As can be seen in the figure, a decrease in β by a factor of 10^{-6} , with γ adjusted to fix the point at which the curves cross, has only a small effect on the quality of the fit to the data. Further decrease in β has little effect on the length of the plateau. We conclude that the cooperativity is required to explain the presence of a long induction time.

One advantage of the microscopic approach is that, as discussed in the Appendix, the size distribution of the clusters is easily calculated. The number of clusters with radius R

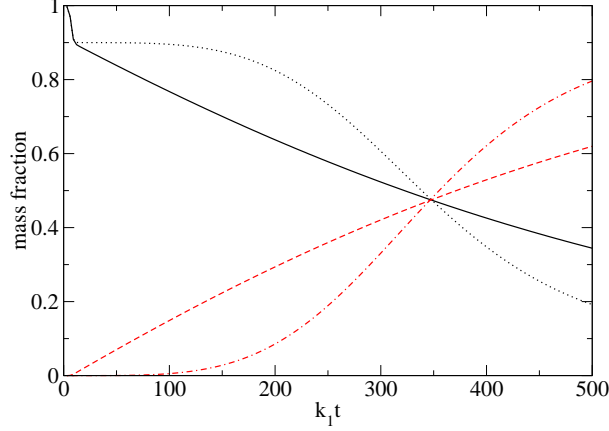


FIG. 5: (Color on line) Comparison of the model without cooperativity and the data. The solid and dotted lines are the nanoparticle mass fractions and the remaining curves are the solid mass fraction. The solid and dashed lines were calculated using $\beta = 5.0$ and $\gamma = 0.0034k_1$; the dotted and dash-dotted lines correspond to $\beta = 5 \times 10^{-6}$ and $\gamma = 2.66k_1$. Decreasing β gives a slightly longer plateau but never as long and sharp as that possible when cooperativity is present.

or smaller at time t , $\mathcal{N}(R, t)$, is given by

$$\mathcal{N}(R, t) = \begin{cases} 0, & \text{if } R \leq R_0 \\ \frac{M}{m_0}(\tilde{\mathcal{N}}(u(t)) - \tilde{\mathcal{N}}(u(t) + 1 - \frac{R}{R_0})), & \text{if } R_0 < R < R_0(u(t) + 1) \\ \frac{M}{m_0}\tilde{\mathcal{N}}(u(t)), & \text{if } R \geq (u(t) + 1)R_0 \end{cases}$$

The function $\tilde{\mathcal{N}}(u)$ is related to the total number of clusters by $\mathcal{N}(t) = \frac{M}{m_0}\tilde{\mathcal{N}}(u(t))$ and is closely related to $\tilde{s}(u)$. Its explicit form is

$$\tilde{\mathcal{N}}(u) = \sum_{j=1}^D a_j \exp(\lambda_j u). \quad (4.18)$$

The factor $R_0(u(t) + 1)$ occurring in the size distribution is the radius of the largest possible cluster at time t and the prefactor $\frac{M}{m_0}$ is the maximum number of clusters that could be created from the given amount of material.

V. CONCLUSION

We have shown that a self-organization process involving self-assembly/nucleation, growth and cooperativity mediated by intermediates consisting of a polydisperse popula-

tion of nanosized particles with varying structure accounts for the kinetics of self-assembly observed in a class of nano-sized materials. In particular, the models reproduce a long quasi-steady state and the long waiting times observed as well as the final apparent equilibrium between nanoparticles and clusters of final product. Note that the reason for the termination of the self-assembly process in our model is due to the depletion of the particles, X . At some point, the $N \rightarrow X$ transitions can not compensate for the fast incorporation of X into the final phase. As new particles can only be formed when some X is already present, the whole process stops when X is fully consumed. The model that we have introduced may account for a broad class of aggregation processes. There is evidence that the complex mechanism of zeolite synthesis, at least some features of it, can be described by this model. The two-step behavior of Fig. 2-a resembles the evolution of particle populations as depicted in Figs. 3 and 4, especially if we assume that some part of the (larger) intermediates X belong to the undetected (solid) phase. Moreover, the extinction of structured nanoparticles/intermediates which announces the end of the growth process, seems confirmed by experiment (compare Q^4 in Fig. 2-d with $X(t)$ in Figs. 3 and 4).

The basic physical mechanisms were modeled at two levels. First, a purely phenomenological model was presented which captures the basic ideas in their simplest form. Then, a more detailed and mechanistic picture was given. This involved new concepts, such as the distribution of cluster sizes, but in the end was reduced to a system of rate equations similar to the first model. In fact, it was noted that the phenomenological model could be viewed as a systematic approximation to the more detailed model.

It was shown that the concept of cooperativity plays a key role in explaining the observations. When cooperativity is removed from the model, it is not possible to simultaneously reproduce the long waiting time at the beginning of the process and the rapid growth that occurs after long times.

One point that deserves emphasis is the limited nature of the assumptions underlying our model. It is based on analogies to the familiar ideas of crystallization³⁹ but we do not claim that the processes are necessarily the same. The nucleation event that initializes crystallization in a simple fluid is probably a much simpler process than the self-assembly in more complex materials such as zeolites. However, it makes sense that in both cases the rate at which the process happens must surely, in a first approximation, be proportional to the supersaturation. Similarly, the mechanism of cooperativity in a simple fluid is simply

the accelerating growth of crystallites as they become larger. In some cases, secondary nucleation on growing crystals is also a factor. In zeolites, however, it may be a true catalysis of the transformation of intermediaries from one form to another. Whatever the nanoscale mechanism, it is plausible that in a first approximation the rate must be proportional to the surface area of existing clusters and to the supersaturation. Our results strongly suggest that some form of cooperativity, whose specifics will depend on the system at hand, is necessary when long induction times precede rapid transformation from one state to another.

It would be interesting to compare the results of our model with other experimental data³⁶ and theoretical models that have been proposed⁴² for zeolites. Moreover, it is hoped that this model will provide a framework for pursuing further experiments. In particular, the model makes a definite prediction concerning the distribution of cluster sizes and it would seem that this could be checked via experiment.

Acknowledgments

This work was supported in part by the Prodex programme of the European Space Agency under contract number C90241. CEAK, TSvE, and JAM acknowledge the Flemish government for long-term structural support via the centre of excellence (CECAT), the concerted research action (GOA), and Methusalem funding. TPC and AA were supported by an IWT and FWO grant respectively.

Appendix A: Elaboration of the model of Section IV

1. Derivation of eqns (4.11-4.16)

The model for the formation of solid can be summarized as

$$\begin{aligned}
 s(t) &= M^{-1} \int_0^t m(t, t') \frac{d\mathcal{N}(t')}{dt'} dt' \\
 \frac{dm(t, t')}{dt} &= k_g x A(t, t') \\
 \frac{d\mathcal{N}(t)}{dt} &= M k_n x + k_a x \int_0^t A(t, t') \frac{d\mathcal{N}(t')}{dt'} dt'
 \end{aligned} \tag{A.1}$$

The mass and surface area of a growing cluster will be related in a system-specific way. For example, if the cluster is spherical, then the area will scale as the square of the radius and the mass as its cube. On the other hand, if the growth is primarily one-dimension, e.g. a cylinder which grows by becoming longer, then the mass and area will both increase in time as the first power of the length. We will assume in general that there is some length scale, $R(t, t')$ characterizing the size of clusters at time t' which have nucleated at time t and that the area scales as $A(t, t') = G_A R^{D-1}(t, t')$, where G_A is a geometric factor and D is the dimensionality of the growth process so that the mass will scale as $m(t, t') = \rho G_V L^D(t, t')$. Then, the equations for the mass and number become

$$\begin{aligned} \frac{dR(t, t')}{dt} &= \frac{k_g G_A}{D \rho G_v} x, \quad R(t, t) = R_0 \\ \frac{d\mathcal{N}(t)}{dt} &= M k_n x + G_A k_a x \int_0^t R^D(t, t') \frac{d\mathcal{N}(t')}{dt'} dt', \end{aligned} \quad (\text{A.2})$$

Note that the initial radius is related to the initial mass of a cluster by where $m_0 = \rho G_V R_0^D$. Next, introduce the variable $u(t) = \frac{R(t, 0) - R_0}{R_0}$. From

$$R(t, t') = R_0 + \frac{k_g G_A}{D \rho G_v} \int_{t'}^t x(t'') dt''$$

we derive the following expression

$$R(t, t') = R(t, 0) - R(t', 0) + R_0 = (u(t) - u(t') + 1) R_0$$

From

$$\frac{du}{dt} = \frac{1}{R_0} \frac{dR(t, 0)}{dt} = \frac{k_g G_A}{D \rho G_v} x(t) \equiv \gamma x(t)$$

and

$$\frac{dx}{dt} = \nu_1(n, x) - \frac{ds}{dt} = \nu_1(n, x) - \frac{ds}{du} \frac{du}{dt}$$

we have already derived eqns [4.11] and [4.16]. However, we still need to prove eqns (4.12-4.15).

Notice that the radius increases monotonically with time. We can therefore replace time by $u(t)$ and write $\mathcal{N}(t) = \frac{M}{m_0} \tilde{\mathcal{N}}(u(t))$ for some function $\tilde{\mathcal{N}}$, (the prefactor being introduced to simplify later expressions). Using $\frac{d\mathcal{N}}{dt} = \frac{M}{m_0} \frac{d\tilde{\mathcal{N}}}{du} \frac{du}{dt}$, the equation for the number of clusters can be rearranged to give

$$\frac{d\tilde{\mathcal{N}}(u)}{du} = \beta + \alpha \int_0^u (u - u' + 1)^{D-1} \frac{d\tilde{\mathcal{N}}(u')}{du'} du' \quad (\text{A.3})$$

with

$$\alpha = \frac{DG_V k_a \rho R_0^D}{k_g} = \frac{D k_a m_0}{k_g}, \quad \beta = \frac{m_0 DG_V \rho R_0 k_n}{G_A k_g} \quad (\text{A.4})$$

An integration by parts gives

$$\frac{d\tilde{\mathcal{N}}(u)}{du} = \beta + \alpha \tilde{\mathcal{N}}(u) + (D-1) \alpha \int_0^u (u-u'+1)^{D-2} \tilde{\mathcal{N}}(u') du'. \quad (\text{A.5})$$

where we assumed $\tilde{\mathcal{N}}(0) = 0$ as there is no solid present at $t = 0$. Continuing to differentiate gives

$$\begin{aligned} \frac{d^2 \tilde{\mathcal{N}}(u)}{du^2} &= \alpha \frac{d\tilde{\mathcal{N}}(u)}{du} + \alpha (D-1) \tilde{\mathcal{N}}(u) \\ &\quad + \alpha \frac{(D-1)!}{(D-3)!} \int_0^u (u-u'+1)^{D-3} \tilde{\mathcal{N}}(u') du' \\ \frac{d^3 \tilde{\mathcal{N}}(u)}{du^3} &= \alpha \frac{d^2 \tilde{\mathcal{N}}(u)}{du^2} + \alpha (D-1) \frac{d\tilde{\mathcal{N}}(u)}{du} \\ &\quad + \alpha \frac{(D-1)!}{(D-3)!} \tilde{\mathcal{N}}(u) \\ &\quad + \alpha \frac{(D-1)!}{(D-4)!} \int_0^u (u-u'+1)^{D-4} \tilde{\mathcal{N}}(u') du' \end{aligned} \quad (\text{A.6})$$

where we used that

$$\frac{d}{dx} \int_a^x f(x, y) dy = f(x, x) + \int_a^x \frac{df(x, y)}{dx} dy \quad (\text{A.7})$$

for any function f and constant a . The original integral equation is therefore equivalent to a simple D -order differential,

$$\frac{d^D \tilde{\mathcal{N}}(u)}{du^D} = \alpha \sum_{j=1}^D \frac{(D-1)!}{(D-j)!} \frac{d^{D-j} \tilde{\mathcal{N}}(u)}{du^{D-j}} \quad (\text{A.8})$$

equation with boundary conditions

$$\begin{aligned} \tilde{\mathcal{N}}(0) &= 0, \quad \left. \frac{d\tilde{\mathcal{N}}(u)}{du} \right|_0 = \beta \\ \left. \frac{d^j \tilde{\mathcal{N}}(u)}{du^j} \right|_0 &= \alpha \sum_{i=1}^{j-1} \frac{(D-1)!}{(D-i)!} \left. \frac{d^{j-i} \tilde{\mathcal{N}}(u)}{du^{j-i}} \right|_0, \quad j = 2 \dots D-1 \end{aligned} \quad (\text{A.9})$$

The solution is a sum of exponentials,

$$\tilde{\mathcal{N}}(u) = \sum_{j=1}^D a_j \exp(\lambda_j u), \quad (\text{A.10})$$

where the constants λ_i are the roots of

$$\lambda^D - \alpha \sum_{j=1}^D \frac{(D-1)!}{(D-j)!} \lambda^{D-j} = 0 \quad (\text{A.11})$$

Using Eq.(A.9), the coefficients satisfy

$$\begin{aligned} 0 &= \sum_{j=1}^D a_j \\ \beta &= \sum_{j=1}^D \lambda_j a_j, \text{ if } D > 1 \\ \alpha\beta &= \sum_{j=1}^D \lambda_j^2 a_j, \text{ if } D > 2 \end{aligned} \quad (\text{A.12})$$

and so on. In general, solution for the coefficients requires solving this system. For example, for the most interesting cases of $D = 2$ and $D = 3$, the solution is

$$\begin{aligned} a_i &= \beta \frac{1}{2\lambda_i - \lambda_1 - \lambda_2}, \quad D = 2 \\ a_i &= \beta \frac{\alpha - \sum_{j \neq i} \lambda_j}{\prod_{j \neq i} (\lambda_i - \lambda_j)}, \quad D = 3 \end{aligned} \quad (\text{A.13})$$

Finally, the mass fraction of solid is

$$\begin{aligned} s(t) &= M^{-1} \int_0^t m(t, t') \frac{d\mathcal{N}(t')}{dt'} dt' \\ &= \frac{G_V \rho}{m_0} R_0^3 \int_0^{u(t)} (u(t) - u' + 1)^D \frac{d\tilde{\mathcal{N}}(u')}{du'} du' \end{aligned} \quad (\text{A.14})$$

or $s(t) = \tilde{s}(u(t))$ with

$$\tilde{s}(u) = \int_0^u (u - u' + 1)^D \frac{d\tilde{\mathcal{N}}(u')}{du'} du' \quad (\text{A.15})$$

as $G_V \rho R_0^3 / m_0 = 1$. Differentiating gives

$$\frac{d}{du} \tilde{s}(u) = \frac{d\tilde{\mathcal{N}}(u)}{du} + D \int_0^u (u - u' + 1)^{D-1} \frac{d\tilde{\mathcal{N}}(u')}{du'} du' \quad (\text{A.16})$$

Substituting from eqn (A.3),

$$\frac{d}{du} \tilde{s}(u) = \frac{d\tilde{\mathcal{N}}(u)}{du} + \frac{D}{\alpha} \left(\frac{d\tilde{\mathcal{N}}(u)}{du} - \beta \right) \quad (\text{A.17})$$

giving

$$\tilde{s}(u) = \left(1 + \frac{D}{\alpha} \right) \tilde{\mathcal{N}}(u) - D \frac{\beta}{\alpha} u. \quad (\text{A.18})$$

Insertion of eqn (A.10) into eqn (A.18) results in eqn (4.12).

2. Derivation of eqn (4.17)

In order to make contact with the phenomenological model, it is useful to develop the solution for the mass fraction as a power series. From eqn (A.6) and the boundary conditions, it is easily shown that

$$\tilde{\mathcal{N}}(u) = \sum_{n=0}^{\infty} c_n u^n \quad (\text{A.19})$$

with

$$\begin{aligned} c_0 &= 0, \quad c_1 = \beta, \quad c_2 = \frac{1}{2}\alpha\beta, \quad \text{and for } n \geq 3 \\ c_n &= \frac{\alpha}{n}c_{n-1} + \frac{2\alpha}{n(n-1)}c_{n-2} + \frac{2\alpha}{n(n-1)(n-2)}c_{n-3}. \end{aligned} \quad (\text{A.20})$$

Thus,

$$\begin{aligned} \tilde{s} &= \left(1 + \frac{3}{\alpha}\right) \sum_{n=1}^{\infty} c_n u^n - 3\frac{\beta}{\alpha}u \\ &= \beta u + \frac{1}{2}\beta(\alpha+3)u^2 + \frac{1}{6}\beta(\alpha+3)(\alpha+2)u^3 + \dots \end{aligned} \quad (\text{A.21})$$

We can invert this power series using Lagrange inversion theorem which states that

$$u(s) = \sum_{n=1}^{\infty} \frac{n-1}{u^{n-1}} \left(\frac{u}{s(u)} \right)^n \bigg|_{u=0} \frac{s^n}{n!} \quad (\text{A.22})$$

and results in

$$u = \frac{1}{\beta}\tilde{s} - \frac{(\alpha+3)}{2\beta^2}\tilde{s}^2 + \frac{(2\alpha+7)(\alpha+3)}{6\beta^3}\tilde{s}^3 + \dots$$

Finally, to fully eliminate u in favor of s we need

$$\begin{aligned} \frac{d}{du}\tilde{s}(u) &= \beta + \beta(\alpha+3)u + \frac{1}{2}\beta(\alpha+3)(\alpha+2)u^2 + \dots \\ &= \beta + (\alpha+3)\tilde{s} - \frac{1}{2}\frac{(\alpha+3)}{\beta}\tilde{s}^2 + \dots \end{aligned} \quad (\text{A.23})$$

Substitution of this relation into the model, eqn (4.11), gives the rate-like form, eqn (4.17).

3. Size distribution

Let $\mathcal{N}(R, t)$ be the number of clusters of radius R or smaller. Since the clusters grow monotonically, a cluster of radius R at time t was nucleated at some definite time $t'(R) < t$.

Hence, the total number of clusters with radius less than R is the total number of clusters minus the number with radius greater than R which is to say the total number minus the number already present at time $t'(R)$,

$$\mathcal{N}(R, t) = [\mathcal{N}(t) - \mathcal{N}(t'(R))] \Theta(R_m(t) - R) \Theta(R - R_0) \quad (\text{A.24})$$

where the step function $\Theta(R - R_0)$ enforces the condition that there are no clusters smaller than R_0 and the step function $\Theta(R_m(t) - R)$ is required since there is a maximal size corresponding to a cluster nucleated at time $t = 0$ (assuming there are no clusters present at $t < 0$). Hence, when $R > R_m$, $\mathcal{N}(R, t)$ is simply equal to the total number of clusters $\mathcal{N}(t)$. Now, the problem is to find $t'(R)$. It is sufficient to note that $R = R(t, t') = (u(t) - u(t') + 1) R_0$. Since $\mathcal{N}(t'(R)) = \frac{M}{m_0} \tilde{\mathcal{N}}(u(t'(R))) = \frac{M}{m_0} \tilde{\mathcal{N}}\left(u + 1 - \frac{R}{R_0}\right)$. It then follows that

$$\mathcal{N}(R, t) = \Theta(R - R_0) \frac{M}{m_0} \times \left(\tilde{\mathcal{N}}(u(t)) - \tilde{\mathcal{N}}\left(u(t) + 1 - \frac{R}{R_0}\right) \Theta(R_m(t) - R) \right) \quad (\text{A.25})$$

Finally, note that R_m is found by taking $t' = 0$ giving $R_m = R(t, 0) = (u(t) + 1) R_0$ so that

$$\mathcal{N}(R, t) = \Theta(R - R_0) \frac{M}{m_0} \times \left(\tilde{\mathcal{N}}(u(t)) - \tilde{\mathcal{N}}\left(u(t) + 1 - \frac{R}{R_0}\right) \Theta((u(t) + 1) R_0 - R) \right) \quad (\text{A.26})$$

This expression simply means that the number of clusters of size R or smaller is the total number of clusters created since the time $t'(R)$ at which clusters of size R were created.

4. No cooperativity

The limit of no cooperativity, $k_a = \alpha = 0$, is not easy to extract from the general solution. A simpler approach is to return to eqn (A.3) which, in this limit, becomes

$$\frac{d\mathcal{N}(t)}{dt} = M k_n x = M k_n \gamma^{-1} \frac{du}{dt} = \frac{M \rho R_0 k_n}{k_g} \frac{du}{dt} \quad (\text{A.27})$$

or

$$\frac{d \frac{m_0}{M} \mathcal{N}(t)}{dt} = \frac{d \tilde{\mathcal{N}}(t)}{dt} = \frac{m_0 \rho R_0 k_n}{k_g} \frac{du}{dt} = \beta \frac{du}{dt}$$

so that $\tilde{\mathcal{N}}(u) = \beta u$. Substituting this into the result for the size distribution gives

$$\mathcal{N}(R, t) = \beta \left(\frac{M}{m_0} \right) \Theta(R - R_0) \times \left(u(t) - \left(u(t) + 1 - \frac{R}{R_0} \right) \Theta((u(t) + 1) R_0 - R) \right) \quad (\text{A.28})$$

The total mass fraction can now be calculated since the mass of a cluster of radius R is simply $G_V R^D \rho$ and the number of clusters with radius between R and $R + dR$ is $\frac{dn(R, t)}{dR} dR$ and $\frac{dn(R, t)}{dR} = \beta \frac{M}{m_0} \frac{1}{R_0} \Theta(R - R_0) \Theta((u(t) + 1) R_0 - R)$. Summing over all radii gives

$$\begin{aligned} s(t) &= \frac{1}{M} \int_0^\infty G_V R^D \rho \frac{d\mathcal{N}(R, t)}{dR} dR \\ &= \beta \frac{1}{M} \left(\frac{M}{m_0} \right) \int_{R_0}^{(u(t)+1)R_0} \frac{1}{R_0} G_V R^D \rho dR \\ &= \frac{\beta}{D+1} \left((u(t) + 1)^{D+1} - 1 \right) \end{aligned} \quad (\text{A.29})$$

In this limit, our result thus reduces to a form that occurs in the theory of crystallization³⁹.

* Electronic address: E-mail: jlutsko@ulb.ac.be

† Electronic address: E-mail: Titus.VanErp@biw.kuleuven.be

¹ G. Nicolis, Self-Organization in Nonequilibrium Systems (John Wiley and Sons, New York, 1977).

² R. D. Sudduth, P. K. Yarala, and Q. Sheng, *Polymer Engineering and Science* **42**, 694 (2002).

³ M. C. Vanderleeden, D. Kashchiev, and G. M. Vanrosmalen, *J. Crystal Growth* **130**, 21 (1993).

⁴ M. Muchova and F. Lednický, *J. Macromolecular Science-Physics* **334**, 55 (1995).

⁵ F. Lednický and M. Muchova, *J. Macromolecular Science-Physics* **224**, 75 (1995).

⁶ O. Galkin and P. G. Vekilov, *J. Mol. Bio.* **336**, 43 (2004).

⁷ O. Galkin, R. L. Nagel, and P. G. Vekilov, *J. Mol. Bio.* **365**, 425 (2007).

⁸ O. Galkin, W. Pan, L. Filobelo, R. E. Hirsch, R. L. Nagel, and P. G. Vekilov, *Biophysical Journal* **93**, 902 (2007).

⁹ D. W. Oxtoby, *Nature* **420**, 277 (2002).

¹⁰ V. Talanquer and D. W. Oxtoby, *J. Chem. Phys.* **109**, 223 (1998).

- ¹¹ V. Basios, J. Lutsko, G. Nicolis, D. Maes, and C. Kirschhock, *Microgravity Science and Technology* **21**, 47 (2009).
- ¹² J. F. Lutsko and G. Nicolis, *Phys. Rev. Lett.* **96**, 046102 (2006).
- ¹³ J. J. Kozak, C. Nicolis, and G. Nicolis, *J. Chem. Phys.* **126**, 154701 (2007).
- ¹⁴ R. Barrer, "Hydrothermal chemistry of zeolites" (Academic Press, London, 1982).
- ¹⁵ C. E. A. Kirschhock, S. P. B. Kremer, J. Vermant, G. V. Tendeloo, P. A. Jacobs, and J. A. Martens, *Chem. Eur. J.* **11**, 4306 (2005).
- ¹⁶ S. Kremer, C. Kirschhock, A. Aerts, K. Villani, J. Martens, O. Lebedev, and G. V. Tendeloo, *Adv. Mater. Weinheim* **15**, 1705 (2003).
- ¹⁷ S. Kremer, E. Theunissen, C. Kirschhock, J. Martens, P. Jacons, and W. Herfs, *Adv. Space Res.* **32**, 2003 (259).
- ¹⁸ M. G. Clerici, *Top. Catal.* **13**, 373 (2000).
- ¹⁹ S. Eslava, F. Iacopi, M. R. Baklanov, C. E. A. Kirschhock, K. Maex, and J. A. Martens, *J. Am. Chem. Soc.* **129**, 9288 (2007).
- ²⁰ E. M. Flanigen, J. M. Bennett, R. W. Grose, J. P. Cohen, R. L. Patton, R. M. Kirchner, and J. V. Smith, *Nature* **271**, 512 (1978).
- ²¹ J. N. Watson, L. E. Iton, R. I. Keir, J. C. Thomas, T. L. Dowling, and J. W. White, *J. Phys. Chem. B* **101**, 10094 (1997).
- ²² B. J. Schoeman, *Zeolites* **18**, 97 (1997).
- ²³ B. J. Schoeman, *Microporous Mater.* **9**, 267 (1997).
- ²⁴ P. P. E. A. de Moor, T. P. M. Beelen, and R. A. van Santen, *J. Phys. Chem. B* **103**, 1639 (1999).
- ²⁵ P. P. E. A. de Moor, T. P. M. Beelen, R. A. van Santen, L. W. Beck, and M. E. Davis, *J. Phys. Chem. B* **104**, 7600 (2000).
- ²⁶ S. Mintova, N. H. Olson, J. Senker, and T. Bein, *Angew. Chem. Int. Ed.* **41**, 2558 (2002).
- ²⁷ C. J. Y. Houssin, C. E. A. Kirschhock, P. C. M. M. Magusin, B. L. Mojet, P. J. Grobet, P. A. Jacobs, J. A. Martens, and R. A. van Santen, *Phys. Chem. Chem. Phys.* **5**, 3518 (2003).
- ²⁸ J. M. Fedeyko, J. D. Rimer, R. F. Lobo, and D. G. Vlachos, *J. Phys. Chem. B* **108**, 12271 (2004).
- ²⁹ J. D. Rimer, D. G. Vlachos, and R. F. Lobo, *J. Phys. Chem. B* **109**, 12762 (2005).
- ³⁰ S. A. Pelster, W. Schrader, and F. Schuth, *J. Am. Chem. Soc.* **128**, 4310 (2006).

- ³¹ T. M. Davis, T. O. Drews, H. Ramanan, C. He, J. Dong, H. Schnablegger, M. A. Katsoulakis, E. Kokkoli, A. V. McCormick, R. L. Penn, et al., *Nat. Mater.* **5**, 400 (2006).
- ³² A. Patis, V. Dracopoulos, and V. Nikolakis, *J. Phys. Chem. C* **111**, 17478 (2007).
- ³³ A. Aerts, L. Follens, M. Haouas, T. Caremans, M.-A. Delsuc, B. Loppinet, J. Vermant, B. Goderis, F. Taulelle, J. Martens, et al., *Chem. Mater.* **19**, 3448 (2007).
- ³⁴ L. Follens, A. Aerts, M. Haouas, T. Caremans, B. Loppinet, B. Goderis, J. Vermant, F. Taulelle, J. Martens, and C. Kirschhock, *Phys. Chem. Chem. Phys.* **10**, 5574 (2008).
- ³⁵ J. L. Provis, J. D. Gehman, C. E. White, and D. G. Vlachos, *J. Phys. Chem. C* **112**, 14769 (2008).
- ³⁶ A. Aerts, M. Haouas, T. P. Caremans, L. R. A. Follens, T. S. van Erp, F. Taulelle, J. Vermant, J. A. Martens, and C. E. A. Kirschhock, *Chemistry - A European Journal* **16**, 2794 (2010).
- ³⁷ D. Kashchiev, Nucleation (Butterworth-Heinemann, Oxford, 2000).
- ³⁸ P. Jensen, *Rev. Mod. Phys.* **71**, 1695 (1999).
- ³⁹ J. W. Mullin, Crystallization (Butterworth, Oxford, 1997).
- ⁴⁰ M. Ausloos and M. Dirickx, eds., The Logistic Map and the Route to Chaos (Springer, Berlin, 2006).
- ⁴¹ J. C. Groen, G. M. Hamminga, J. A. Moulijn, and J. Perez-Ramirez, *Phys. Chem. Chem. Phys.* **9**, 4822 (2007).
- ⁴² T. O. Drews and M. Tsapatsis, *Microporous Mesoporous Mat.* **101**, 97 (2007).